Cell Reports

Article

Quality-controlled ceramide-based GPI-anchored protein sorting into selective ER exit sites

Graphical abstract

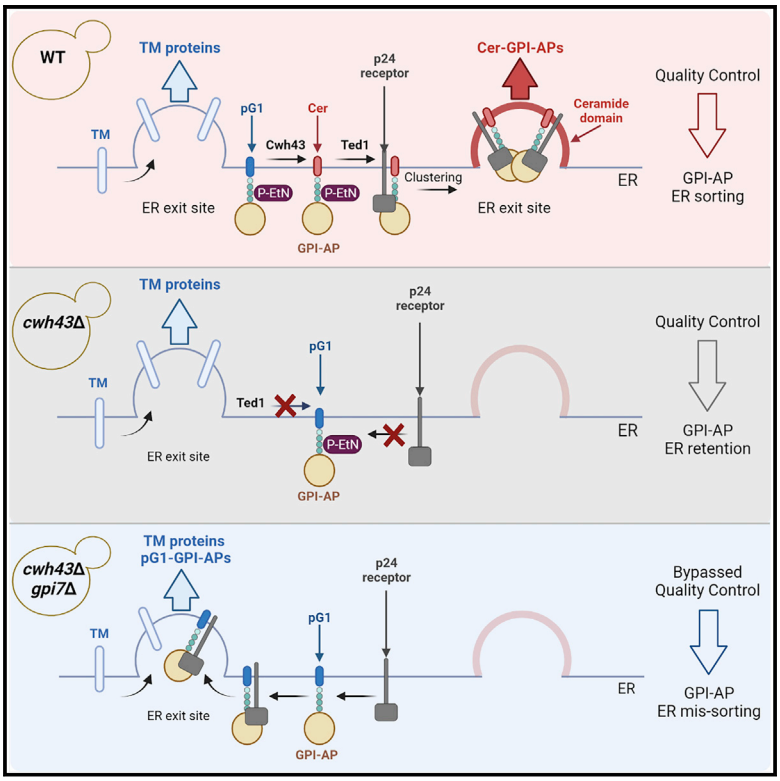

Highlights

- Ceramide moiety of GPI-anchor is required for clustering and ER exit of GPI-APs
- GPI-AP with ceramide moiety is monitored by the GPI-glycan remodelase Ted1
- GPI ceramide remodeling is required for sorting of GPI-APs into selective ERESs
- Lipid-based protein sorting is quality controlled in the ER membranes

Authors

Sofia Rodriguez-Gallardo, Susana Sabido-Bozo, Atsuko Ikeda, ..., Kazuo Kurokawa, Manuel Muñiz, Kouichi Funato

Correspondence

kkurokawa@riken.jp (K.K.), mmuniz@us.es (M.M.), kfunato@hiroshima-u.ac.jp (K.F.)

In brief

GPI-APs undergo remodeling before exiting the ER. Rodriguez-Gallardo et al. show that GPI-APs remodeled with a very-long acyl chain ceramide moiety are monitored by a GPI-glycan remodelase. This quality-control system is necessary to ensure the lipid-based sorting of GPI-APs into selective ERESs for differential ER export.

Rodriguez-Gallardo et al., 2022, Cell Reports *39*, 110768
May 3, 2022
https://doi.org/10.1016/j.celrep.2022.110768

CellPress

Cell Reports

CellPress
OPEN ACCESS

Article

Quality-controlled ceramide-based GPI-anchored protein sorting into selective ER exit sites

Sofia Rodriguez-Gallardo,[1,4] Susana Sabido-Bozo,[1,4] Atsuko Ikeda,[2,4] Misako Araki,[2] Kouta Okazaki,[2] Miyako Nakano,[2] Auxiliadora Aguilera-Romero,[1] Alejandro Cortes-Gomez,[1] Sergio Lopez,[1] Miho Waga,[3] Akihiko Nakano,[3] Kazuo Kurokawa,[3,*] Manuel Muñiz,[1,*] and Kouichi Funato[2,5,*]

[1]Department of Cell Biology, Faculty of Biology, University of Seville and Instituto de Biomedicina de Sevilla (IBiS), Hospital Universitario Virgen del Rocío/CSIC/Universidad de Sevilla, 41012 Seville, Spain

[2]Graduate School of Integrated Sciences for Life, Hiroshima University, Higashi-Hiroshima, Hiroshima 739-8528, Japan

[3]Live Cell Super-Resolution Imaging Research Team, RIKEN Center for Advanced Photonics, Wako, Saitama 351-0198, Japan

[4]These authors contributed equally

[5]Lead contact

*Correspondence: kkurokawa@riken.jp (K.K.), mmuniz@us.es (M.M.), kfunato@hiroshima-u.ac.jp (K.F.)

https://doi.org/10.1016/j.celrep.2022.110768

SUMMARY

Glycosylphosphatidylinositol-anchored proteins (GPI-APs) exit the endoplasmic reticulum (ER) through a specialized export pathway in the yeast *Saccharomyces cerevisiae*. We have recently shown that a very-long acyl chain (C26) ceramide present in the ER membrane drives clustering and sorting of GPI-APs into selective ER exit sites (ERES). Now, we show that this lipid-based ER sorting also involves the C26 ceramide as a lipid moiety of GPI-APs, which is incorporated into the GPI anchor through a lipid-remodeling process after protein attachment in the ER. Moreover, we also show that a GPI-AP with a C26 ceramide moiety is monitored by the GPI-glycan remodelase Ted1, which, in turn, is required for receptor-mediated export of GPI-APs. Therefore, our study reveals a quality-control system that ensures lipid-based sorting of GPI-APs into selective ERESs for differential ER export, highlighting the physiological need for this specific export pathway.

INTRODUCTION

Lipidation is an essential post-translational modification by which proteins are covalently modified with specific lipids that regulate protein localization, function, and stability. Glycosylphosphatidylinositol (GPI) anchoring is a special type of lipidation present in all eukaryotes that occurs at the endoplasmic reticulum (ER) and targets GPI-anchored proteins (GPI-APs) to the cell surface, where they play a range of essential physiological roles (Kinoshita et al., 2013; Muñiz and Riezman, 2016; Lopez et al., 2019; Kinoshita, 2020). The core structure of the GPI-anchor precursor is largely conserved in evolution and consists of a phospholipid moiety (acylphosphatidylinositol) with a glycan backbone [(EtNP)Man3-(EtNP)Man2-(EtNP)Man1-GlcN], where EtNP is a side-branch ethanolamine-phosphate, Man is mannose (the numbers represent the positions of the Man in the anchor), and GlcN is glucosamine. Once the GPI-anchor precursor has been made by a series of sequential reactions at the ER membrane, it is then attached *en bloc* in the ER lumen by a GPI-transamidase complex to newly synthesized proteins containing a GPI attachment signal sequence at their C terminus.

Immediately after GPI attachment and during GPI-AP secretory transport to the cell surface, the lipid moiety of the GPI anchor undergoes structural remodeling, which is important for GPI-AP function and trafficking (Tanaka et al., 2004; Bosson et al., 2006; Fujita et al., 2006a, 2006b; Maeda et al., 2007; Fujita and Jigami, 2008; Fujita and Kinoshita, 2012; Kinoshita and Fujita. 2016). In yeast, lipid remodeling entirely occurs at the ER (Figure 1A), with an inositol deacylation by Bst1 followed by fatty-acid remodeling, which involves the removal of an unsaturated fatty acid at the sn2 position by Per1 and its replacement with a very-long chain saturated fatty acid (C26) by Gup1 (Bosson et al., 2006; Fujita et al., 2006a, 2006b). In most cases, the C26 diacylglycerol (DAG), formed as part of the anchor, is replaced with a ceramide that also contains a very-long chain saturated fatty acid (C26), by Cwh43 (Conzelmann et al., 1992; Reggiori et al., 1997; Ghugtyal et al., 2007; Umemura et al., 2007). In addition to the GPI lipid remodeling, the glycan portion of the GPI anchor also undergoes another remodeling process prior to ER exit (Fujita et al., 2009; Manzano-Lopez et al., 2015). The initial side-chain EtNP on the second mannose of the glycan portion is removed by the specific phosphodiesterase Ted1 (Manzano-Lopez et al., 2015). The remodeled GPI glycan is then recognized by the transmembrane cargo receptor p24 complex, which, in turn, selectively recruits Lst1, a specific isoform of the major COPII cargo binding subunit Sec24 required to form GPI-AP-enriched COPII vesicles (Manzano-Lopez et al., 2015).

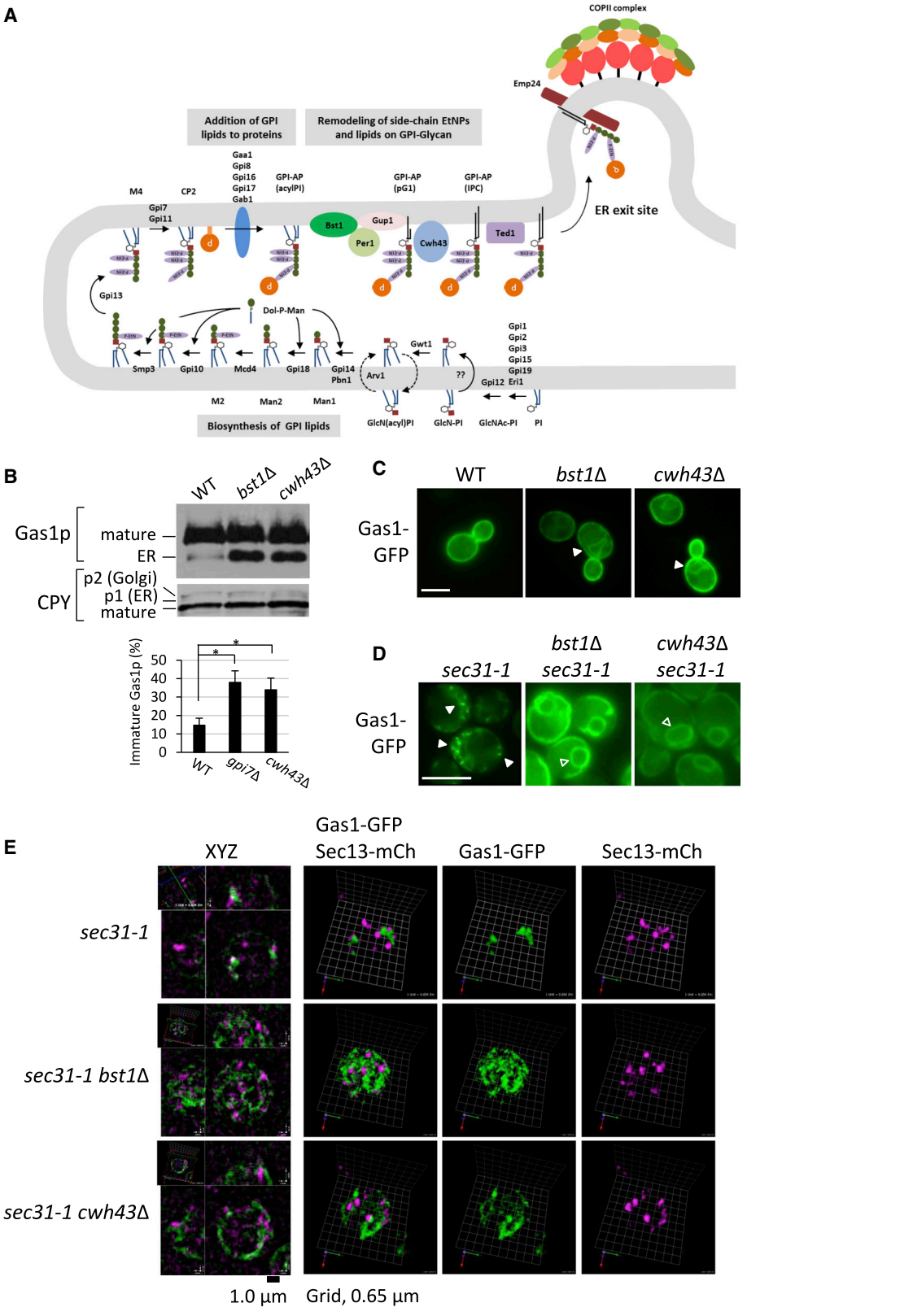

(legend on next page)

While in mammals, the Golgi complex is the site where GPI-APs are sorted from other secretory proteins, in yeast, the ER is the major sorting station. Although how the difference is made remains unknown, clustering of GPI-APs seems to be one of the determinants of this sorting process (Lebreton et al., 2019; Rodriguez-Gallardo et al., 2020). In yeast, GPI-APs having a C26 ceramide lipid moiety are clustered into discrete ER zones associated with specific ER exit sites (ERESs) (Rodriguez-Gallardo et al., 2020). This clustering and subsequent sorting process are hindered by decreasing the acyl chain length of free ceramide in the membrane from C26 to C16-C18. These data indicate that the chain length of ceramide in the ER membrane is critical for the sorting of GPI-APs and is consistent with a model by which C26 ceramides and GPI-APs having C26 ceramide can be cotransported to the Golgi in the same specialized COPII vesicles (Kajiwara et al., 2008; Loizides-Mangold et al., 2012; Muñiz and Riezman, 2016; Funato et al., 2020). It is, however, unclear whether GPI lipid remodeling is involved in the sorting of GPI-APs or in how ceramide-based GPI-AP sorting into ERESs is regulated.

Here, we investigated the role of a lipid moiety of GPI-APs in its sorting process and demonstrated that ceramide remodeling is required for clustering and subsequent sorting of GPI-APs. In addition, biochemical analyses revealed that a GPI-AP with a C26 ceramide moiety remodeled by Cwh43 is monitored by the GPI-glycan remodelase Ted1 to ensure recognition by the p24 complex and ER export of GPI-APs with C26 ceramide, providing a mechanism by which GPI-AP cargo sorting is quality controlled in the ER membranes. Our data provide insight into the physiological role of the ceramide moiety of GPI-APs on GPI-AP sorting.

RESULTS

ER clustering of Gas1 is driven by GPI ceramide remodeling

Gas1 is a GPI-AP that has a C26 ceramide as a GPI lipid moiety (Yoko-O et al., 2013; Rodriguez-Gallardo et al., 2020). In a previous study, deletion of *CWH43* was shown to cause accumulation of the ER form of Gas1 (Yoko-O et al., 2013; Yoko-O et al., 2018). We confirmed and showed that, like in *bst1*Δ mutant cells, the ER form of Gas1 was accumulated in *cwh43*Δ cells (Figure 1B), suggesting that ceramide remodeling of GPI anchors is required for the efficient ER-to-Golgi transport of GPI-APs. By contrast, the maturation of carboxypeptidase Y (CPY), a non-GPI-AP, was not affected in the *bst1*Δ or *cwh43*Δ cells (Figure 1B). Consistent with this, we observed that deletion of either *BST1* or *CWH43* retains Gas1-GFP in the ER, as is evident from the ER-characteristic nuclear ring staining (Figure 1C). These findings led to the idea that ceramide remodeling might contribute to sorting of GPI-APs into ERESs.

We have recently shown that very-long acyl chain ceramides present in the ER membrane drive clustering and subsequent sorting of newly synthesized Gas1 tagged with GFP into selective ERESs (Rodriguez-Gallardo et al., 2020). Therefore, we tested whether Gas1-GFP is aggregated into clusters in *cwh43*Δ mutant cells. For this purpose, we used the temperature-sensitive COPII allele *sec31-1* as a genetic tool to reversibly retain newly synthesized cargo proteins at the ER. Gas1-GFP concentration and cluster formation at the ER membranes can be observed in the *sec31-1* mutant cells under fluorescence microscopy by inhibiting COPII vesicle budding at a restrictive temperature (37°C) and releasing the budding block upon shifting down to a low temperature (24°C), as recently established (Rodriguez-Gallardo et al., 2020). Gas1-GFP was clustered in *sec31-1* mutant cells, but it was mainly unclustered and distributed throughout the ER membrane in *sec31-1 cwh43*Δ like in *sec31-1 bst1*Δ (Figure 1D). In addition, analysis using super-resolution confocal live imaging microscopy (SCLIM) also confirmed that Gas1-GFP was unclustered in the lipid-remodeling mutant cells and showed that Gas1-GFP clusters in the *sec31-1* mutant cells were adjacent to ERESs labeled with Sec13-mCherry (Figure 1E) (Rodriguez-Gallardo et al., 2020).

Figure 1. Ceramide remodeling is required for clustering of GPI-APs in ER membranes

(A) A scheme for the overall GPI-AP biosynthetic pathway. The pathway can be divided into three parts: biosynthesis of the GPI anchor, attachment of the GPI anchor to protein, and remodeling of GPI-APs. After the attachment of the GPI anchor to protein, structural remodeling occurs on the lipid and glycan portions of the GPI anchor. The acyl chain linked to inositol is removed by Bst1. Then, the unsaturated fatty acyl chain within the sn2 position is eliminated by Per1 and replaced with a long saturated (C26:0) fatty acid by Gup1 followed by the replacement of the diacylglycerol (DAG) moiety by ceramides, a reaction that requires Cwh43. Side-chain ethanolamine phosphate (EtNP) residue attached to the second mannose is removed by a phosphodiesterase Ted1, and GPI-APs exit the ER in COPII-coated vesicles through direct interaction with the Emp24 complex as a cargo receptor.

(B and C) Lipid remodeling is required for efficient ER-to-Golgi transport of Gas1, a ceramide-based GPI-AP. Deletion of *BST1* or *CWH43* causes accumulation of the ER form of Gas1.

(B) Extracts prepared from wild-type and mutant cells were analyzed by western blot for Gas1 and CPY. Mature, mature forms of Gas1 and CPY; ER, immature ER form of Gas1; p1 and p2, ER and Golgi forms of CPY, respectively. Quantification of the percentage of immature Gas1 was performed. The bars represent the average of three independent biological replicates. Statistics: error bars indicate the SD. Student's t test. *$p < 0.05$.

(C) Gas1-GFP localization in wild-type and deletion mutant cells was analyzed by conventional fluorescence microscopy. Scale bar, 5 μm.

(D and E) Newly synthesized Gas1-GFP forms clusters in the wild-type ER membrane adjacent to specific ERESs but not in the *bst1*Δ or *cwh43*Δ mutant ER membrane.

(D) *sec31-1*, *sec31-1 bst1*Δ, and *sec31-1 cwh43*Δ cells expressing galactose-inducible Gas1-GFP (green) and constitutive ERES marker Sec13-mCherry (ERES, magenta) were incubated at 37°C for 30 min and then shifted down to 24°C to release a secretion block and imaged by conventional fluorescence microscopy after 20 min. White arrowheads: ER Gas1-GFP clusters; open arrowheads: unclustered Gas1-GFP distributed throughout the ER membrane showing the ER-characteristic nuclear ring staining. Scale bar, 5 μm.

(E) The same strains as in (D) were incubated at 37°C for 30 min, shifted down to 24°C to release a secretion block, and imaged by SCLIM after 20 min. Left panels show representative merged two-dimensional (2D) images of Gas1-GFP and Sec13-mCherry at one xyz plane. Scale bar, 1 μm. Right panels show representative merged 3D images of Gas1-GFP and Sec13-mCherry. Scale unit, 0.65 μm. Gas1-GFP was detected in discrete ER zones or clusters adjacent to specific ERESs in wild-type cells. Gas1-GFP was unclustered in lipid-remodeling-deficient mutant cells.

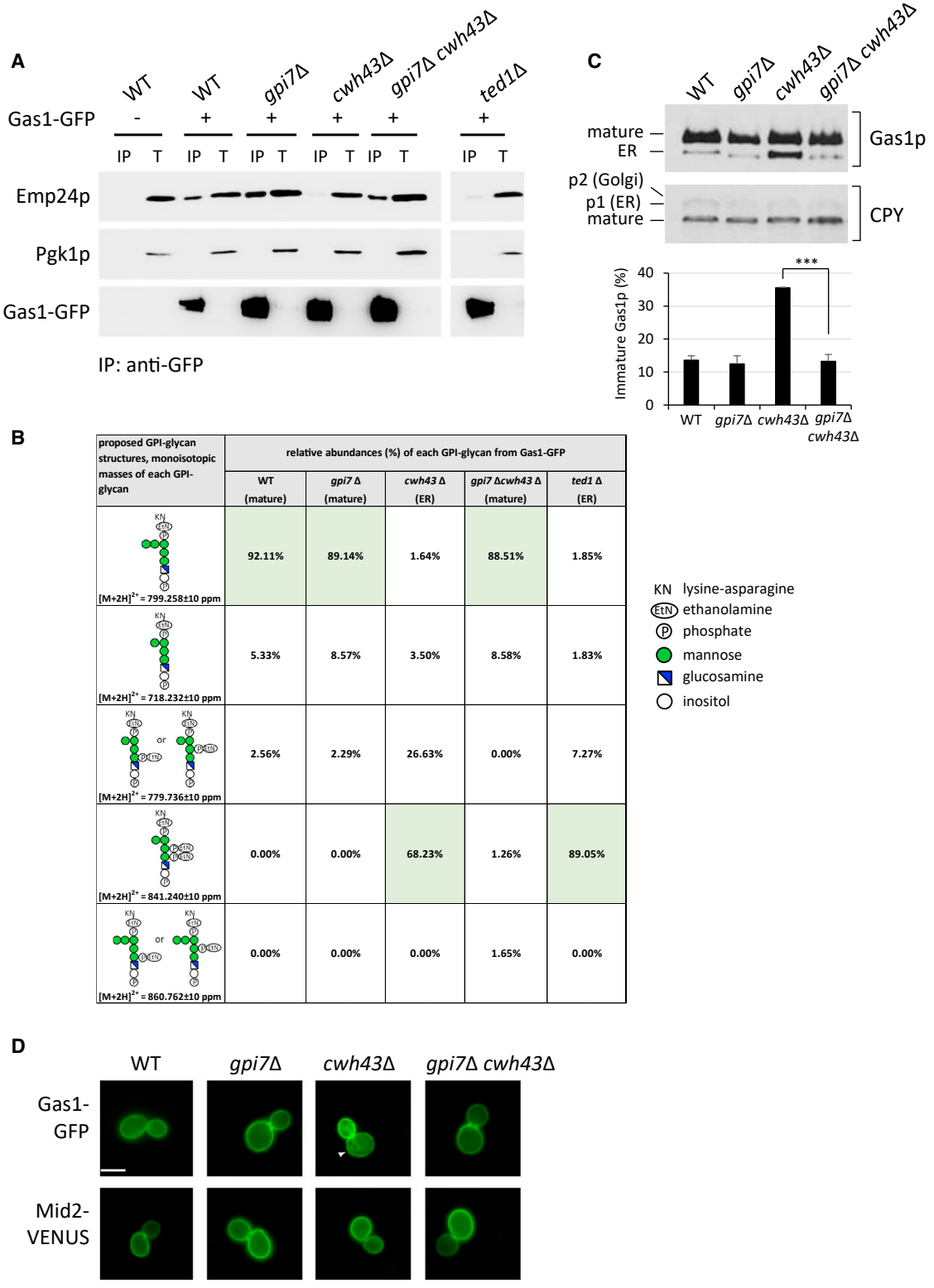

Figure 2. EtNP trimming is required for ceramide-remodeling-dependent association of Gas1p with p24 complex and ER export of Gas1

(A) Coimmunoprecipitation (coIP) assay between Gas1-GFP and the p24 complex subunit Emp24. *gpi7*Δ bypasses the requirement of Cwh43 for the association of Gas1 with p24 complex. Gas1-GFP is specifically recognized by the p24 complex in a Cwh43-dependent manner. This physical interaction is specific because Pgk1, an unrelated cytosolic protein, is not associated with Gas1-GFP after IP, and the *gpi7*Δ mutation suppresses the defect in an interaction between

(legend continued on next page)

These results demonstrate that ceramide remodeling of the GPI anchors is required for ER clustering of Gas1.

Gas1 with a C26 ceramide moiety is monitored by the GPI-glycan remodelase Ted1 to ensure ER export

As Gas1-GFP clustering at the ER requires removal of EtNP from the second mannose residue in GPI anchors by Ted1 and subsequent recognition by the transmembrane cargo receptor p24 complex (Rodriguez-Gallardo et al., 2020), GPI ceramide remodeling by Cwh43 could be indirectly required for Gas1 clustering through p24 binding. Therefore, we addressed whether Gas1 could bind with the p24 complex in *cwh43*Δ by examining the extent of interaction between Gas1-GFP and Emp24, a component of the p24 complex. As a negative control, we used *ted1*Δ mutant cells in which the interaction between GPI-APs and Emp24 is disrupted (Manzano-Lopez et al., 2015). As shown in Figure 2A, in *ted1*Δ mutant cells, Emp24 did not coprecipitate with Gas1-GFP, whereas wild-type cells exhibited an association of Emp24 with Gas1-GFP. By using this method, we found that Emp24 could not be efficiently coprecipitated with Gas1-GFP in the *cwh43*Δ cells, suggesting that GPI ceramide remodeling is required for the recognition of Gas1 by the p24 complex. Furthermore, this binding defect observed in *cwh43Δ* cells was rescued by the additional deletion of *GPI7* (*gpi7*Δ *cwh43*Δ). Since *GPI7* encodes an enzyme that adds the EtNP on the second mannose during GPI anchor biosynthesis that is later removed by Ted1, the loss of function of Gpi7 leads to the production of GPI anchors without the EtNP on the second mannose (Benachour et al., 1999). Therefore, the binding rescue by *gpi7* mutation suggests that the Emp24-binding defect in *cwh43*Δ cells could be due to the inability of Ted1 to trim the second EtNP. We then addressed this possibility by mass spectrometry analysis of the GPI glycan of Gas1-GFP. Most of the peptides bearing GPI glycan from the mature Gas1-GFP in wild-type and *gpi7*Δ mutant cells had no side-chain EtNP attached to mannose (m/z 799.258 corresponding to KN-EtNP-Man(Man-Man)-Man-Man-GlcN-Ino-P), whereas GPI glycan from the immature Gas1-GFP in the *cwh43*Δ or *ted1*Δ cells had two side-chain EtNPs (m/z = 841.240 corresponding to KN-EtNP-Man(Man)-Man(EtNP)-Man(EtNP)-GlcN-Ino-P) (Figure 2B). Therefore, these findings confirm that Ted1 only acts once the GPI anchor of Gas1 has been remodeled to ceramide by Cwh43.

If ER export of Gas1 is dependent on the trimming of the second EtNP and subsequent recognition by the p24 complex, the ER-export defect in *cwh43*Δ cells should be rescued by the *gpi7*Δ mutation because the Emp24-binding defect in *cwh43*Δ was suppressed by deleting *GPI7* (Figure 2A). As seen in Figure 2C, deletion of *GPI7* suppressed the accumulation of the ER form of Gas1 caused by the *cwh43*Δ mutation. Gas1-GFP retained in the ER of *cwh43*Δ was also diminished by the *gpi7*Δ mutation (Figure 2D). These data are consistent with the model that ceramide remodeling is required for clustering and ER export of Gas1 through the trimming of EtNP in GPI anchors. Consistently, the role of ceramide remodeling is specific for GPI-APs because transport of non-GPI-anchored cargo, CPY (Figure 2C) or Mid2-VENUS (Figure 2D), was not affected in *cwh43*Δ cells. Taken together, these results suggest that glycan remodelase Ted1 monitors GPI-AP with a ceramide moiety remodeled by Cwh43 to ensure that exported Gas1 has ceramide as a GPI lipid moiety.

We have recently shown that the chain length of ceramide in the ER membrane is critical for the clustering and sorting of Gas1 remodeled with C26 ceramide (Rodriguez-Gallardo et al., 2020). This is consistent with a model in which free ceramides and ceramide-based GPI-APs are cotransported in the same vesicles to the Golgi (Kajiwara et al., 2008; Loizides-Mangold et al., 2012; Muñiz and Riezman, 2016; Funato et al., 2020). Since deletion of *GPI7* suppressed the ER accumulation of unremodeled GPI-APs, we next analyzed if the free-ceramide requirement for ER exit of GPI-APs can be restored by the *gpi7*Δ mutation. For this purpose, we used myriocin, a specific inhibitor of serine palmitoyltransferase (SPT), that is the enzyme catalyzing in the first step in sphingolipid synthesis (Horvath et al., 1994). We observed that in myriocin-treated wild-type cells, Gas1 and Gas1-GFP but not non-GPI-APs (CPY, Mid2-VENUS) accumulated in the ER, whereas in myriocin-treated *gpi7*Δ cells, the GPI-APs were not localized to the ER (Figures 3A and 3B). Similar results were obtained with temperature-sensitive *lcb1-100* mutant background strains (Figure 3C), which are defective in SPT at a non-permissive temperature (37°C) (Zanolari et al., 2000). These results indicate that removal of EtNP from the second mannose overrides not only ceramide remodeling but also the free-ceramide requirement for ER exit of GPI-APs.

When *GPI7* is deleted, the retention of Gas1 in the ER caused by *emp24*Δ was not rescued (Figures 4A and 4B). Similar results were obtained in *arv1*Δ defective in GPI-anchor synthesis (Kajiwara et al., 2008) (Figure 4C), *bst1*Δ, or *gup1*Δ (Figure 4D). Therefore, the ceramide-bypass pathway in the absence of EtNP on the second mannose requires remodeling of the GPI anchor to C26 DAG, in addition to recognition by the p24 complex, because the *gup1*Δ mutant is deficient in the generation of a pG1-type anchor consisting of C26 DAG (Bosson et al., 2006; Fujita et al., 2006a; Umemura et al., 2007; Ghugtyal et al., 2007).

Gas1-GFP and the p24 complex caused by the deletion of *CWH43*. Enriched ER fractions of wild-type and mutant cells expressing Gas1-GFP were processed for native IP. Bound material (IP) was resolved by SDS-PAGE and analyzed by immunoblotting using antibodies against Emp24, Pgk1, and GFP. Total (T) represents a fraction of the solubilized input material.

(B) Structural analysis of the GPI glycan of Gas1-GFP. Extracts prepared from cells expressing Gas1-GFP were treated with PI-specific phospholipase C (PI-PLC), and then Gas1-GFP was purified, digested with trypsin, and analyzed by liquid chromatography electrospray ionization tandem mass spectrometry (LC-ESI-MS/MS). The table shows the percentage of different GPI-glycan structures found in the mature or ER forms of Gas1-GFP purified from wild-type and mutant cells. The relative abundance (%) of each GPI glycan was calculated from the peak intensity of monoisotopic masses of each GPI glycan.

(C and D) *gpi7*Δ mutation suppresses the accumulation of the ER form of Gas1 caused by the *cwh43*Δ mutation.

(C) Extracts prepared from cells were analyzed by western blot for Gas1 and CPY as in Figure 1B. Quantification of the percentage of immature Gas1 was performed. The bars represent the average of three independent biological replicates. Error bars indicate the SD. Statistics: Student's t test. ***$p < 0.001$.

(D) Localization of Gas1-GFP and Mid2-VENUS was analyzed by conventional fluorescence microscopy. Scale bar, 5 μm.

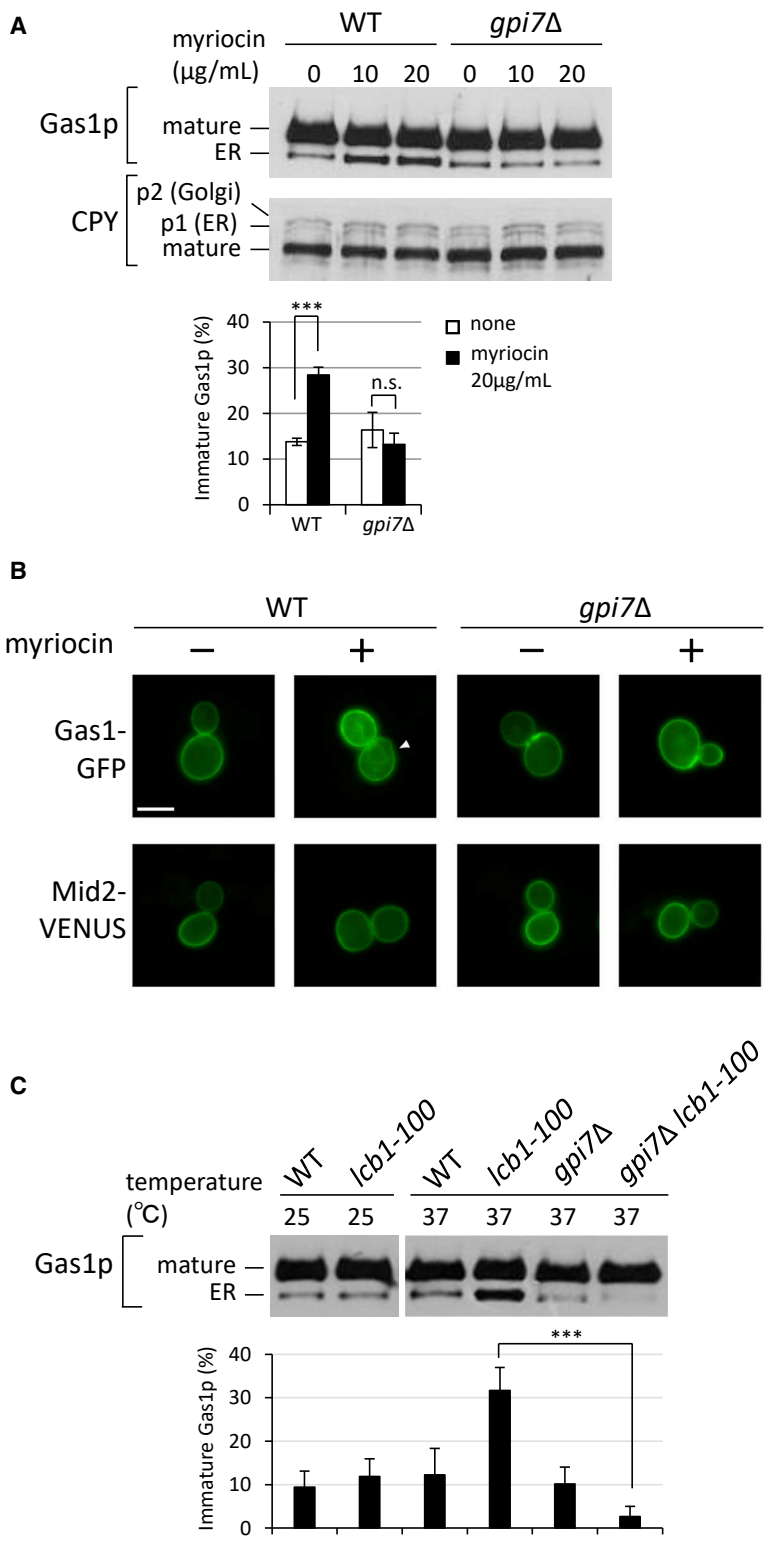

Figure 3. Elimination of EtNP attached to second mannose bypasses ceramide-dependent transport of GPI-APs

(A–C) *gpi7*Δ mutation suppresses the accumulation of the ER form of Gas1 caused by inhibition of sphingolipid synthesis.

(A) Extracts prepared from cells treated with indicated concentration of myriocin were analyzed by western blot for Gas1 and CPY as in Figure 1B. Quantification of the percentage of immature Gas1 was performed. The bars represent the average of three independent biological replicates. Error bars indicate the SD. Statistics: Student's t test. n.s., not significant, and ***$p < 0.001$.

(B) Localization of Gas1-GFP and Mid2-VENUS in the cells treated with or without myriocin (10 μg/mL, for 1.5 h at 24°C) was analyzed by conventional fluorescence microscopy. Scale bar, 5 μm.

(C) Cells grown at 25°C were shifted to 25°C or 37°C for 120 min, and the extracts prepared from the cells were analyzed by western blot for Gas1 as in Figure 1B. Quantification of the percentage of immature Gas1 was performed. The bars represent the average of three independent biological replicates. Error bars indicate the SD. Statistics: Student's t test. ***$p < 0.001$.

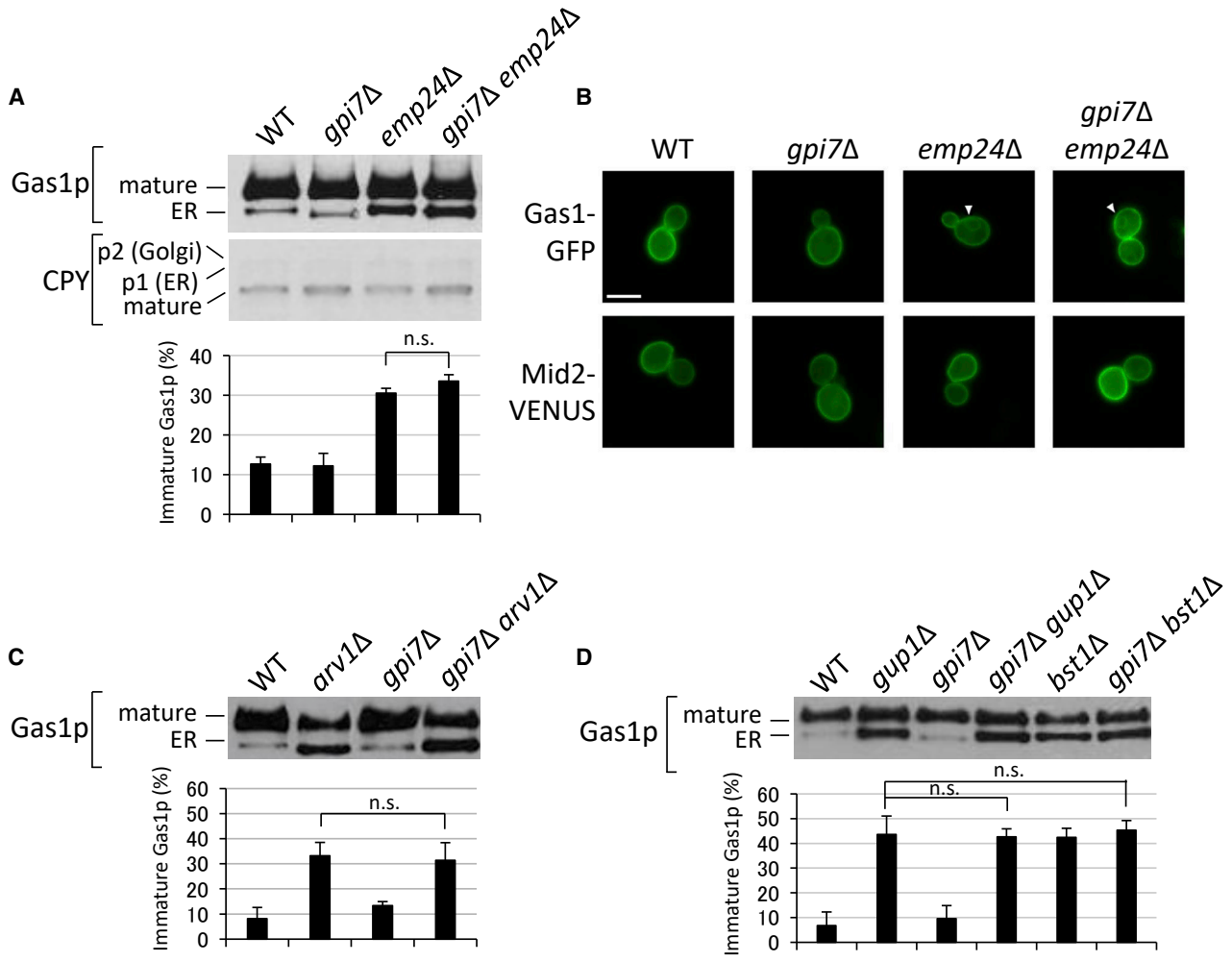

Figure 4. ER export of GPI-APs in *gpi7*Δ requires GPI anchoring, PI with a C26:0 fatty-acid moiety, and p24 complex

(A, C, and D) Extracts prepared from wild-type and mutant cells were analyzed by western blot for Gas1 (A, C, and D) and CPY (A) as in Figure 1B. Quantification of the percentage of immature Gas1 was performed. The bars represent the average of three independent biological replicates. Error bars indicate the SD. Statistics: Student's t test. n.s., not significant.

(B) Localization of Gas1-GFP and Mid2-VENUS was analyzed by conventional fluorescence microscopy. Scale bar, 5 μm.

Gas1 sorting into selective ERESs depends on GPI ceramide remodeling

We have recently shown that Gas1-GFP and the transmembrane plasma membrane protein Mid2-iRFP are segregated into different ERESs during ER export (Rodriguez-Gallardo et al., 2020). In addition, the data presented in the previous paragraph show that *GPI7* mutation, which generates GPI-APs with C26 DAG-based GPI (Benachour et al., 1999; Fujita et al., 2006a; Umemura et al., 2007), bypasses the Ted1 requirement for p24-dependent ER export of Gas1. Therefore, we took advantage of the *gpi7*Δ mutant to address whether GPI ceramide remodeling is required for sorting of Gas1, since C26 DAG-based Gas1 in *cwh43*Δ mutant cells was unclustered (Figures 1D and 1E). Thus, we constructed single (*sec31-1*), double (*sec31-1 gpi7*Δ), and triple (*sec31-1 gpi7*Δ *cwh43*Δ) mutants of *sec31-1*, *gpi7*Δ, and *cwh43*Δ expressing Gas1-GFP and Mid2-iRFP with the COPII outer coat protein Sec13 tagged with mCherry. We then analyzed them by SCLIM and quantified the proportion of ERESs in which only one type of cargo or both are present (Figures 5A and 5B). SCLIM analysis showed that after incubation at 37°C and subsequent release at 24°C for 20 min, most of the ERESs (about 75%) contained only one type of cargo in *sec31-1* mutant cells. The top panels of Figure 5A show typical examples of ERESs with only one cargo in *sec31-1* mutant cells. About 15% of ERESs contained both cargos overlapping in the same area (Figures 5A, yellow filled arrowheads), and 10% of ERESs contained both cargos but segregated in clearly distinct zones. These results indicate that Gas1-GFP is sorted into different ERESs from Mid2-iRFP upon ER exit. Most importantly, we found that in either *sec31-1 gpi7*Δ or *sec31-1 gpi7*Δ *cwh43*Δ mutant cells, a large percentage of ERESs (40%) include both cargos overlapping in the same area, and the percentage of

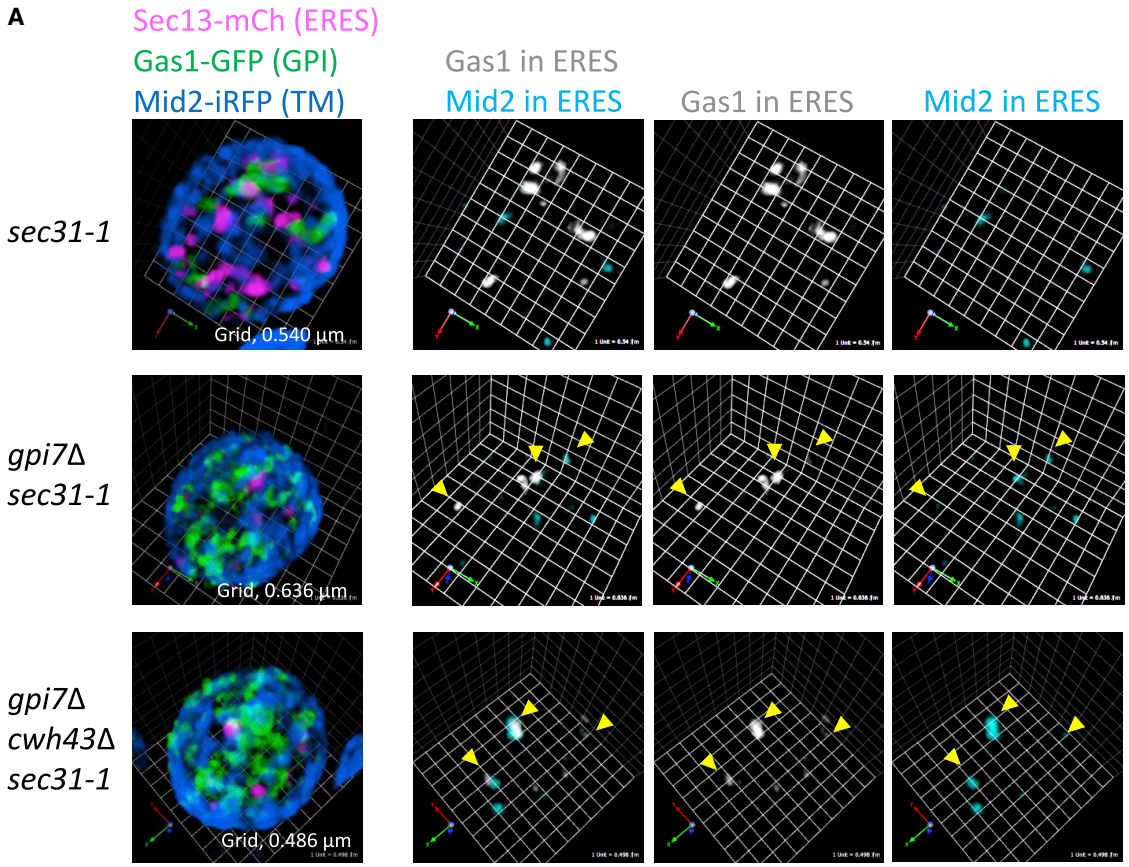

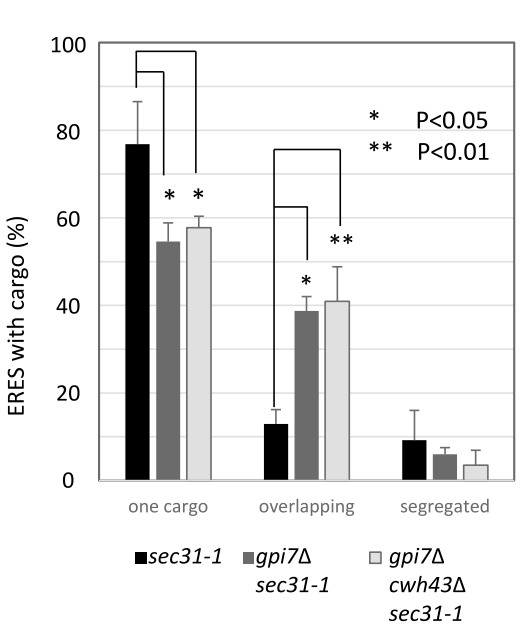

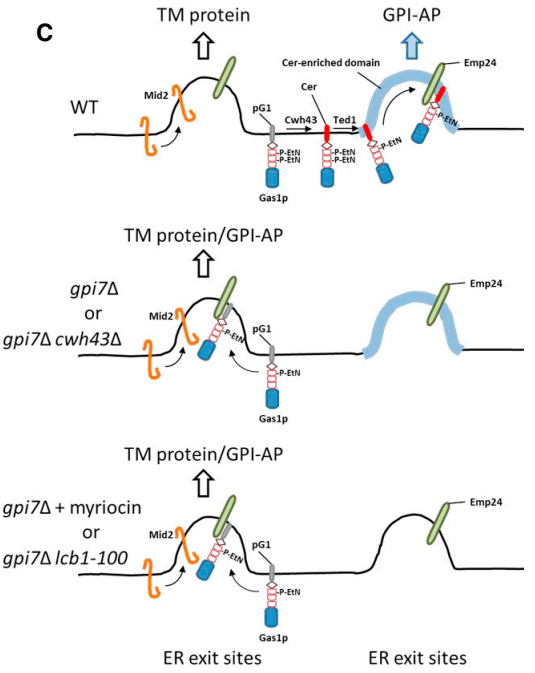

(legend on next page)

ERESs with only one type of cargo is reduced (Figure 5B), implying that GPI ceramide remodeling is required for sorting of GPI-APs and also that this lipid-based sorting is controlled by the GPI-glycan remodelase Ted1 (Figure 5C).

DISCUSSION

GPI-APs are segregated from other secretory proteins and sorted into distinct transport vesicles along the secretory pathway (Fujita and Kinoshita, 2012; Kinoshita et al., 2013; Kinoshita and Fujita, 2016; Muñiz and Riezman, 2016; Lopez et al., 2019; Lebreton et al., 2019; Funato et al., 2020). As the GPI moiety of GPI-APs is recognized by the cargo receptor p24 complex, it is postulated to act as a signal for GPI-AP sorting (Muñiz et al., 2000; Takida et al., 2008; Castillon et al., 2009, 2011; Fujita et al., 2011), but the underlying mechanism remains elusive. We have recently shown that GPI-APs having a C26 ceramide lipid moiety are clustered into discrete ER zones associated with specific ERESs and that a very-long acyl chain of ceramide in the membrane is required for their clustering and subsequent sorting (Rodriguez-Gallardo et al., 2020). This suggests that ceramide in the membrane is critical for ER clustering and sorting of GPI-APs with a C26 ceramide lipid moiety. Therefore, it seems that remodeled GPI-APs with a C26 ceramide coalesce with ceramides into ordered domains in the relatively disordered lipid environment of the ER, although the involvement of ceramide remodeling in sorting has not yet been clarified. Here, we provide evidence that the ceramide moiety of GPI-AP Gas1 is required for its clustering and sorting into selective ERESs. Strikingly, Gas1 with a ceramide moiety remodeled by Cwh43 is monitored by the GPI-glycan remodelase Ted1 to ensure recognition by the p24 complex and ER export, suggesting that sorting of GPI-APs with a C26 ceramide moiety is quality controlled in the ER membranes.

Quality control in the secretory pathway initiates at the ER, where newly synthesized proteins enter into an unfolded state, fold and assemble into functional protein complexes, and then interact with COPII subunits or cargo receptors to exit the ER. The canonical ER quality-control system monitors and facilitates protein folding with the outcome of the degradation of misfolded proteins (Ellgaard and Helenius, 2003; Araki and Nagata, 2011; Sun and Brodsky, 2019; Phillips et al., 2020). Terminally misfolded GPI-APs are degraded by ubiquitin- and proteasome-dependent endoplasmic-reticulum-associated protein degradation (ERAD) or in vacuole/lysosomes by a process called rapid ER stress-induced export (RESET) (Fujita and Jigami, 2008; Satpute-Krishnan et al., 2014; Sikorska et al., 2016; Lopez et al., 2019; Kinoshita, 2020; Nakatsukasa, 2021; Lemus et al., 2021). In mammalian cells, N-glycans and their recognition by calnexin participate in protein-folding quality control and the GPI-inositol deacylation of GPI-APs (Liu et al., 2018; Guo et al., 2020). In yeast, GPI-inositol deacylation by Bst1 (Figure 1A) was shown to be involved in the ER protein-folding quality control of GPI-APs (Fujita et al., 2006b). As the subsequent GPI lipid-remodeling steps driven sequentially by Per1, Gup1, and Cwh43 are dependent on prior GPI-inositol deacylation (Ghugtyal et al., 2007), the GPI-inositol deacylation by Bst1 has been proposed to act as a device that switches GPI-APs from protein folding to ER exit (Fujita et al., 2006b; Fujita and Jigami, 2008). In *gpi7*Δ mutant cells, GPI-inositol deacylation is unaffected (Fujita et al., 2006a; Umemura et al., 2007), suggesting that the EtNP on the second mannose of GPI anchors is not involved in the switching of GPI-APs from protein folding to ER exit. Accordingly, newly synthesized Gas1 and the steady-state levels of hemagglutinin (HA)-Gas1 expressed in wild-type and *cwh43*Δ mutant cells are reduced with the same degradation kinetics (Figure S1). These data indicate that unremodeled GPI-APs produced in the *cwh43*Δ mutant are not cleared by degradation in the ER, unlike terminally misfolded proteins, suggesting that ceramide remodeling is not involved in protein-folding quality control. The fact that Gpi7 facilitates ceramide remodeling (Benachour et al., 1999; Fujita et al., 2006a; Umemura et al., 2007), which is recognized by the GPI-glycan remodelase Ted1, implies that attachment by Gpi7 and trimming by Ted1 of the EtNP on the second mannose function as a quality-control system that monitors the ceramide remodeling of the GPI anchor to ensure the ceramide-based sorting of GPI-APs into selective ERESs for differential ER export from other cargo proteins but not to degrade unremodeled GPI-APs. We propose that, under normal conditions, this ceramide quality-control mechanism might facilitate ER sorting

Figure 5. In *gpi7*Δ cells, Gas1-GFP enters into the same ERESs as transmembrane cargo Mid2-iRFP

(A and B) *sec31-1*, *gpi7*Δ *sec31-1*, and *gpi7*Δ *cwh43*Δ *sec31-1* cells expressing galactose-inducible Gas1-GFP (green) and Mid2-iRFP (blue) and constitutive ERES marker Sec13-mCherry (ERES, magenta) were incubated at 37°C for 30 min and then shifted down to 24°C to release a secretion block and imaged by SCLIM after 20 min.

(A) Left panels show representative merged 3D cell hemisphere images of cargos and ERES markers. Right panels show the same images as in the left panels but processed to display only the cargo (Gas1-GFP, gray, and Mid2-iRFP, light blue) present in the ERESs. The yellow filled arrowheads mark overlapping cargos in ERES.

(B) Quantification of several micrographs described in (A). The graph plots the average percentage of ERESs containing only one cargo (Gas1-GFP or Mid2-iRFP), overlapping cargos, and segregated cargos in *sec31-1*, *gpi7*Δ *sec31-1*, and *gpi7*Δ *cwh43*Δ *sec31-1* cells. n = 238 in 32 cells (*sec31-1*), 423 in 46 cells (*gpi7*Δ *sec31-1*), and 443 in 51 cells (*gpi7*Δ *cwh43*Δ *sec31-1*) in three independent experiments. Error bars indicate the SD. Statistics: two-tailed, unpaired t test. $^{**}p < 0.01$ and $^{*}p < 0.05$.

(C) Model of specific roles of EtNP in sorting of GPI-APs during ER exit. The EtNP attached to the second mannose segregates GPI-APs from transmembrane proteins and concentrates them into specific ERESs by activating ceramide remodelase Cwh43, which remodels a phosphatidylinositol moiety (pG1) of GPI anchors to a very-long-acyl-chain (C26) ceramide moiety (inositolphosphorylceramide [IPC]). The remodeled ceramide-based GPI-APs potentially interact with the very-long-acyl-chain (C26) ceramide-enriched domain, which allows GPI-AP clustering (Rodriguez-Gallardo et al., 2020), and then were sorted into selective ERESs. After the trimming of EtNP by Ted1, the ceramide-based GPI-APs are recognized by the p24 receptor and exit the ER in specialized COPII vesicles. In *gpi7*Δ cells, ceramide remodeling is reduced (Benachour et al., 1999; Fujita et al., 2006a; Umemura et al., 2007), and the GPI-APs bearing pG1 but not EtNP at the second mannose are rerouted to exit the ER with transmembrane proteins via the same ERESs that are used for the export of transmembrane cargo. Recognition by the p24 receptor is still required for ER exit of GPI-APs in the *gpi7*Δ cells.

by delaying the ER exit of those ceramide-based GPI-APs that have not yet been remodeled, giving Cwh43 more time to incorporate the ceramide into their GPI anchor. If this quality-control process is overloaded, as happens in a *cwh43*Δ mutant, unremodeled GPI-APs leak out of the ER via the unspecific bulk flow that slowly transports them to the cell surface through a mis-sorting pathway that could affect the normal cell physiology since GPI-APs are critical for the formation and integrity of the cell wall. Consistently, *cwh43*Δ mutant cells have hypersensitivity to calcofluor white affecting cell-wall integrity (Ram et al., 1994; Umemura et al., 2007). Thus, the role of the ER ceramide-based clustering and sorting of GPI-APs could be to program, from the ER, their functional organization at the plasma membrane.

Biophysical experiments have shown that ceramide has the ability to promote the rigidity and compactness of membranes through the formation of ceramide-rich domains (Goñi and Alonso, 2009; Castro et al., 2014). Furthermore, the properties of these ceramide-rich domains depend on the acyl chain length of the ceramide (Pinto et al., 2011; Ventura et al., 2020; Zelnik et al., 2020). Consistently, our recent study suggested that the ceramide-rich domains formed by very-long acyl chain (C26) membrane ceramides are required for the clustering and sorting of C26 ceramide-based GPI-APs (Rodriguez-Gallardo et al., 2020). In the present study, we showed that in the *cwh43*Δ mutant cells, Gas1 fails to form clusters and to be sorted. In this mutant, the GPI lipid moiety of Gas1 is DAG, containing very-long saturated fatty acids (Yoko-O et al., 2013), but the membrane ceramide is not altered (Figure S2), suggesting that the C26 ceramide moiety in the GPI anchor is also essential for GPI-AP sorting into selective ERESs. Therefore, we propose that the GPI anchor having C26 ceramide can coalesce with the C26 membrane ceramide to form ceramide-rich domains, probably consisting of interdigitated phases that would promote clustering and membrane curvature leading to segregation from transmembrane proteins and formation of budding vesicles, whereas GPI-AP with a DAG moiety is excluded from ceramide-rich domains due to their physical nature, even though the DAG moiety has a saturated and very-long chain. Finally, our previous observation that Ted1 itself is required for Gas1 clustering (Rodriguez-Gallardo et al., 2020) indicates that this process does not play any critical role in the proposed quality control of ceramide-based protein sorting driven by Ted1. Consistently, the specific localization and GPI-glycan remodelase activity of Ted1 are unaffected in cells defective in Gas1 clustering (Figures S3A and S3B) (Rodriguez-Gallardo et al., 2020).

When the second EtNP on GPI is absent, Gas1 with DAG moiety can exit the ER through the route that bypasses ceramide-based GPI-AP transport and enters the same ERES as transmembrane cargo (Figure 5C), This suggests that Ted1 only removes the second EtNP when ceramide is present in Gas1, ensuring the ER export of ceramide containing Gas1 by the p24 complex. Ted1 cannot solely recognize the ceramide moiety since Ted1 also acts on DAG-based GPI-APs as Cwp2 (Manzano-Lopez et al., 2015). This implies that monitoring ceramide remodeling depends on which protein is attached to the GPI anchor. According to this possibility, ceramide- and DAG-based GPI-APs contain a different amino-acid sequence upstream of the GPI-attachment (ω) site, which has been proposed to specifically contribute to differential GPI lipid remodeling and consequently to the destination (plasma membrane or cell wall) (Yoko-O et al., 2018). We speculate that Ted1, in addition to sensing the lipid species of the GPI anchor, must also recognize the protein part of the GPI-AP. In this way, by also recognizing the protein, Ted1 could specifically monitor ceramide remodeling only in ceramide-based proteins like Gas1 but not in DAG-based proteins. Nevertheless, our and previous findings imply that differences in the lipid of GPI-APs contribute to determining sorting of GPI-AP cargos into ERESs and the subsequent final destination of GPI-APs (Yoko-O et al., 2018), which is linked to their biological functions.

Ceramide-based GPI-APs are found in lower eukaryotes such as *Saccharomyces cerevisiae*, *Aspergillus niger*, *Dictyostelium discoideum*, and *Trypanosoma cruzi* (Ferguson et al., 2009) but are not known in mammalian cells. In mammalian cells, most of GPI-APs contain an ether lipid (1-alkyl-2-acyl) phosphatidylinositol (PI) moiety, which is remodeled from the original diacyl PI moiety in the ER during GPI biosynthesis (Kanzawa et al., 2009; Kinoshita 2020). A recent study found that ether lipids and ceramides share some similar physicochemical properties and functions (Jiménez-Rojo et al., 2020). Thus, the ether-lipid moiety in GPI anchors of mammalian cells might act similarly to the ceramide moiety in yeast, as a signal to concentrate GPI-APs to ceramide-rich domains in the ER. Consistently, a biophysical study with artificial membranes has shown that raft-associated mammalian proteins such as GPI-APs are enriched in the highly ordered ceramide-rich domains, while proteins with poor affinity toward the liquid-ordered phase are excluded from them (Chiantia et al., 2008). Importantly, as in yeast, the transport of GPI-APs from the ER to the Golgi is regulated by EtNP trimming by PGAP5 in animal cells (Fujita et al., 2009). Therefore, it is envisaged that lipid (ceramide in yeast and ether lipid in mammal)-based GPI-AP sorting in the ER may be quality controlled by an evolutionary conserved mechanism involving GPI glycan.

Finally, we have shown evidence that clustering and sorting of GPI-APs involve the C26 ceramide as a lipid moiety of GPI-APs, which is incorporated into the GPI anchor through a lipid-remodeling process after protein attachment in the ER and that GPI glycans play an important role in the quality control of ceramide-based GPI-AP sorting. However, whether such a quality-control system exists commonly in eukaryotes and whether it has impacts on the organization and biological activities of GPI-APs at the cell surface remain to be determined.

Limitations of the study

One limitation of our work is that, of the approximately 60 proteins predicted to be modified with GPI in the yeast *Saccharomyces cerevisiae*, the only known GPI-AP with ceramide is Gas1. To date, the only GPI-APs whose lipid portions have been characterized are Gas1 and Cwp2; Gas1 has a ceramide moiety, while Cwp2 does not undergo ceramide remodeling and has a pG1-type lipid moiety (Yoko-O et al., 2013; Yoko-O et al., 2018; Rodriguez-Gallardo et al., 2020). Therefore, whether the quality-control mechanism of ceramide-based GPI-AP sorting described in this study is specific to Gas1 or representative of

GPI-APs with ceramide moiety remains unknown. Although determination of lipid moiety of GPI-APs may be technically challenging, future work will be required to identify GPI-APs with ceramide moiety other than Gas1 and to study the sorting mechanism of their cargo proteins.

Because our studies reveal that both the ceramide moiety of the GPI anchor and C26 ceramide in the membrane are required for ER clustering and sorting of GPI-APs, we proposed that the GPI anchor having C26 ceramide can coalesce with C26 membrane ceramide to form ceramide-rich domains, probably consisting of interdigitated phases that lead to segregation from transmembrane proteins. However, we could not experimentally demonstrate this model. Our claim is therefore a deduction. Further studies using physics-based methods will be required to determine whether GPI-APs with C26 ceramide coalesce with ceramides into ordered domains in artificial membrane vesicles.

In addition, physiological roles of quality-controlled lipid-based protein sorting of GPI-APs remain to be explored. Many genes are known to interact genetically with genes involved in GPI remodeling. A comprehensive analysis with those genes may provide further insight into the role of quality control for GPI-AP sorting.

STAR★METHODS

Detailed methods are provided in the online version of this paper and include the following:

- KEY RESOURCES TABLE
- RESOURCE AVAILABILITY
  - Lead contact
  - Materials availability
  - Data and code availability
- EXPERIMENTAL MODELS AND SUBJECT DETAILS
  - Yeast strains
- METHOD DETAILS
  - Plasmids
  - Culture conditions
  - Immunoblotting
  - Fluorescence microscopy
  - Native coimmunoprecipitation
  - MS analysis of GPI-glycan
  - Lipid labelling with [^{3}H]*myo*-Inositol
  - Pulse-chase analysis
- QUANTIFICATION AND STATISTICAL ANALYSIS
  - Statistical analysis

SUPPLEMENTAL INFORMATION

Supplemental information can be found online at https://doi.org/10.1016/j.celrep.2022.110768.

ACKNOWLEDGMENTS

We thank Laura Popolo for the pRS416-GAS1-GFP plasmid, Howard Riezman for the p415-MID2-VENUS plasmid, Philip Hieter for the pRS416 plasmid, and Yoshifumi Jigami for the pRS305-HA-GAS1 and GFP-HDEL plasmids. This work was funded by the Grants-in-Aid for Scientific Research from Japan Society for the Promotion of Science, Japan (JP19H02922 to M.N. and K.F.; JP25221103, JP17H06420, and JP18H05275 to A.N. and K. K.), by grant PID2020-119505GB-I00/AEI/10.13039/501100011033 to M.M., by grants co-financed by the Junta de Andalucía and the ERDF PY20_01240 and US-1380893 to M.M., and by "VI Own Research Plan" of the University of Seville VIPPIT-2020-I.5 to M.M. This work was also supported by University of Seville fellowships to S.R.-G., a Ministry of Education, Culture, and Sport (MECD) fellowship to S.S.-B., and a "V Own Research Plan" of the University of Seville (VPPI-US) contract (cofounded by the European Social Fund) to S.L. We thank Valeria Zoni and Stefano Vanni for their critical reading of the manuscript. The graphical abstract was created with BioRender.com.

AUTHOR CONTRIBUTIONS

S.R.-G., S.S.-B., A.I., and M.A. designed and constructed strains and plasmids with help from A.A.-R., A.C.-G., S.L., and K.F. S.R.-G., M.W., and K.K. established and performed fluorescent microscopy experiments. S.S.-B., A.I., M.A., A.A.-R., A.C.-G., and S.L. performed biochemical studies and data analysis. S.S.-B., K.O., and M.N. prepared samples for glycan analysis and performed the glycan analysis with help from K.F. K.K., A.N., A.A.-R., M.M., and K.F. designed the experiments and supervised the project. M.M. and K.F. wrote the manuscript with input from all other authors.

DECLARATION OF INTERESTS

The authors declare no competing interests.

Received: October 20, 2021
Revised: February 23, 2022
Accepted: April 11, 2022
Published: May 3, 2022

REFERENCES

Araki, K., and Nagata, K. (2011). Protein folding and quality control in the ER. Cold Spring Harb Perspect. Biol. *3*, a007526. https://doi.org/10.1101/cshperspect.a007526.

Benachour, A., Sipos, G., Flury, I., Reggiori, F., Canivenc-Gansel, E., Vionnet, C., Conzelmann, A., and Benghezal, M. (1999). Deletion of GPI7, a yeast gene required for addition of a side chain to the glycosylphosphatidylinositol (GPI) core structure, affects GPI protein transport, remodeling, and cell wall integrity. J. Biol. Chem. *274*, 15251–15261. https://doi.org/10.1074/jbc.274.21.15251.

Bosson, R., Jaquenoud, M., and Conzelmann, A. (2006). GUP1 of Saccharomyces cerevisiae encodes an O-acyltransferase involved in remodeling of the GPI anchor. Mol. Biol. Cell *17*, 2636–2645. https://doi.org/10.1091/mbc.e06-02-0104.

Castillon, G.A., Aguilera-Romero, A., Manzano-Lopez, J., Epstein, S., Kajiwara, K., Funato, K., Watanabe, R., Riezman, H., and Muñiz, M. (2011). The yeast p24 complex regulates GPI-anchored protein transport and quality control by monitoring anchor remodeling. Mol. Biol. Cell *22*, 2924–2936. https://doi.org/10.1091/mbc.E11-04-0294.

Castillon, G.A., Watanabe, R., Taylor, M., Schwabe, T.M., and Riezman, H. (2009). Concentration of GPI-anchored proteins upon ER exit in yeast. Traffic *10*, 186–200. https://doi.org/10.1111/j.1600-0854.2008.00857.x.

Castro, B.M., Prieto, M., and Silva, L.C. (2014). Ceramide: a simple sphingolipid with unique biophysical properties. Prog. Lipid Res. *54*, 53–67. https://doi.org/10.1016/j.plipres.2014.01.004.

Chiantia, S., Ries, J., Chwastek, G., Carrer, D., Li, Z., Bittman, R., and Schwille, P. (2008). Role of ceramide in membrane protein organization investigated by combined AFM and FCS. Biochim. Biophys. Acta *1778*, 1356–1364. https://doi.org/10.1016/j.bbamem.2008.02.008.

Conzelmann, A., Puoti, A., Lester, R.L., and Desponds, C. (1992). Two different types of lipid moieties are present in glycophosphoinositol-anchored

membrane proteins of Saccharomyces cerevisiae. EMBO J. *11*, 457–466. https://doi.org/10.1002/j.1460-2075.1992.tb05075.x.

Ellgaard, L., and Helenius, A. (2003). Quality control in the endoplasmic reticulum. Nat. Rev. Mol. Cell Biol. *4*, 181–191. https://doi.org/10.1038/nrm1052.

Ferguson, M.A.J., Kinoshita, T., and Hart, G.W. (2009). Glycosylphosphatidylinositol anchors. In Essentials of Glycobiology, 2nd edition, A. Varki, R.D. Cummings, and J.D. Esko, et al., eds. (Cold Spring Harbor (NY): Cold Spring Harbor Laboratory Press), pp. 143–162, Chapter 11.

Fujita, M., and Jigami, Y. (2008). Lipid remodeling of GPI-anchored proteins and its function. Biochim. Biophys. Acta *1780*, 410–420. https://doi.org/10.1016/j.bbagen.2007.08.009.

Fujita, M., and Kinoshita, T. (2012). GPI-anchor remodeling: potential functions of GPI-anchors in intracellular trafficking and membrane dynamics. Biochim. Biophys. Acta *1821*, 1050–1058. https://doi.org/10.1016/j.bbalip.2012.01.004.

Fujita, M., Maeda, Y., Ra, M., Yamaguchi, Y., Taguchi, R., and Kinoshita, T. (2009). GPI glycan remodeling by PGAP5 regulates transport of GPI-anchored proteins from the ER to the Golgi. Cell *139*, 352–365. https://doi.org/10.1016/j.cell.2009.08.040.

Fujita, M., Umemura, M., Yoko-o, T., and Jigami, Y. (2006a). PER1 is required for GPI-phospholipase A2 activity and involved in lipid remodeling of GPI-anchored proteins. Mol. Biol. Cell *17*, 5253–5264. https://doi.org/10.1091/mbc.e06-08-0715.

Fujita, M., Watanabe, R., Jaensch, N., Romanova-Michaelides, M., Satoh, T., Kato, M., Riezman, H., Yamaguchi, Y., Maeda, Y., and Kinoshita, T. (2011). Sorting of GPI-anchored proteins into ER exit sites by p24 proteins is dependent on remodeled GPI. J. Cell Biol *194*, 61–75. https://doi.org/10.1083/jcb.201012074.

Fujita, M., Yoko-O, T., and Jigami, Y. (2006b). Inositol deacylation by Bst1p is required for the quality control of glycosylphosphatidylinositol-anchored proteins. Mol. Biol. Cell *17*, 834–850. https://doi.org/10.1091/mbc.e05-05-0443.

Funato, K., Riezman, H., and Muñiz, M. (2020). Vesicular and non-vesicular lipid export from the ER to the secretory pathway. Biochim. Biophys. Acta Mol. Cell Biol. Lipids *1865*, 158453. https://doi.org/10.1016/j.bbalip.2019.04.013.

Ghugtyal, V., Vionnet, C., Roubaty, C., and Conzelmann, A. (2007). CWH43 is required for the introduction of ceramides into GPI anchors in Saccharomyces cerevisiae. Mol. Microbiol. *65*, 1493–1502. https://doi.org/10.1111/j.1365-2958.2007.05883.x.

Goñi, F.M., and Alonso, A. (2009). Effects of ceramide and other simple sphingolipids on membrane lateral structure. Biochim. Biophys. Acta *1788*, 169–177. https://doi.org/10.1016/j.bbamem.2008.09.002.

Guo, X.Y., Liu, Y.S., Gao, X.D., Kinoshita, T., and Fujita, M. (2020). Calnexin mediates the maturation of GPI-anchors through ER retention. J. Biol. Chem. *295*, 16393–16410. https://doi.org/10.1074/jbc.RA120.015577.

Horvath, A., Sütterlin, C., Manning-Krieg, U., Movva, N.R., and Riezman, H. (1994). Ceramide synthesis enhances transport of GPI-anchored proteins to the Golgi apparatus in yeast. EMBO J. *13*, 3687–3695. https://doi.org/10.1002/j.1460-2075.1994.tb06678.x.

Ikeda, A., Hanaoka, K., and Funato, K. (2021). Protocol for measuring sphingolipid metabolism in budding yeast. STAR Protoc. *2*, 100412. https://doi.org/10.1016/j.xpro.2021.100412.

Ikeda, A., Kajiwara, K., Iwamoto, K., Makino, A., Kobayashi, T., Mizuta, K., and Funato, K. (2016). Complementation analysis reveals a potential role of human ARV1 in GPI anchor biosynthesis. Yeast *33*, 37–42. https://doi.org/10.1002/yea.3138.

Jiménez-Rojo, N., Leonetti, M.D., Zoni, V., Colom, A., Feng, S., Iyengar, N.R., Matile, S., Roux, A., Vanni, S., Weissman, J.S., and Riezman, H. (2020). Conserved functions of ether lipids and sphingolipids in the early secretory pathway. Curr. Biol. *30*, 3775–3787. https://doi.org/10.1016/j.cub.2020.07.059.

Kajiwara, K., Watanabe, R., Pichler, H., Ihara, K., Murakami, S., Riezman, H., and Funato, K. (2008). Yeast ARV1 is required for efficient delivery of an early GPI intermediate to the first mannosyltransferase during GPI assembly and controls lipid flow from the endoplasmic reticulum. Mol. Biol. Cell *19*, 2069–2082. https://doi.org/10.1091/mbc.e07-08-0740.

Kanzawa, N., Maeda, Y., Ogiso, H., Murakami, Y., Taguchi, R., and Kinoshita, T. (2009). Peroxisome dependency of alkyl-containing GPI-anchor biosynthesis in the endoplasmic reticulum. Proc. Natl. Acad. Sci. U S A. *106*, 17711–17716. https://doi.org/10.1073/pnas.0904762106.

Kinoshita, T. (2020). Biosynthesis and biology of mammalian GPI-anchored proteins. Open Biol. *10*, 190290. https://doi.org/10.1098/rsob.190290.

Kinoshita, T., and Fujita, M. (2016). Biosynthesis of GPI-anchored proteins: special emphasis on GPI lipid remodeling. J. Lipid Res. *57*, 6–24. https://doi.org/10.1194/jlr.R063313.

Kinoshita, T., Maeda, Y., and Fujita, M. (2013). Transport of glycosylphosphatidylinositol-anchored proteins from the endoplasmic reticulum. Biochim. Biophys. Acta *1833*, 2473–2478. https://doi.org/10.1016/j.bbamcr.2013.01.027.

Lebreton, S., Paladino, S., and Zurzolo, C. (2019). Clustering in the Golgi apparatus governs sorting and function of GPI-APs in polarized epithelial cells. FEBS Lett. *593*, 2351–2365. https://doi.org/10.1002/1873-3468.13573.

Lemus, L., Matić, Z., Gal, L., Fadel, A., Schuldiner, M., and Goder, V. (2021). Post-ER degradation of misfolded GPI-anchored proteins is linked with microautophagy. Curr. Biol. *31*, 4025–4037. https://doi.org/10.1016/j.cub.2021.06.078.

Liu, Y.S., Guo, X.Y., Hirata, T., Rong, Y., Motooka, D., Kitajima, T., Murakami, Y., Gao, X.D., Nakamura, S., Kinoshita, T., and Fujita, M. (2018). N-Glycan-dependent protein folding and endoplasmic reticulum retention regulate GPI-anchor processing. J. Cell Biol. *217*, 585–599. https://doi.org/10.1083/jcb.201706135.

Loizides-Mangold, U., David, F.P., Nesatyy, V.J., Kinoshita, T., and Riezman, H. (2012). Glycosylphosphatidylinositol anchors regulate glycosphingolipid levels. J. Lipid Res. *53*, 1522–1534. https://doi.org/10.1194/jlr.M025692.

Lopez, S., Rodriguez-Gallardo, S., Sabido-Bozo, S., and Muñiz, M. (2019). Endoplasmic reticulum export of GPI-anchored proteins. Int. J. Mol. Sci. *20*, 3506. https://doi.org/10.3390/ijms20143506.

Maeda, Y., Tashima, Y., Houjou, T., Fujita, M., Yoko-o, T., Jigami, Y., Taguchi, R., and Kinoshita, T. (2007). Fatty acid remodeling of GPI-anchored proteins is required for their raft association. Mol. Biol. Cell *18*, 1497–1506. https://doi.org/10.1091/mbc.e06-10-0885.

Manzano-Lopez, J., Perez-Linero, A.M., Aguilera-Romero, A., Martin, M.E., Okano, T., Silva, D.V., Seeberger, P.H., Riezman, H., Funato, K., Goder, V., et al. (2015). COPII coat composition is actively regulated by luminal cargo maturation. Curr. Biol. *25*, 152–162. https://doi.org/10.1016/j.cub.2014.11.039.

Muñiz, M., Nuoffer, C., Hauri, H.P., and Riezman, H. (2000). The Emp24 complex recruits a specific cargo molecule into endoplasmic reticulum-derived vesicles. J. Cell Biol. *148*, 925–930. https://doi.org/10.1083/jcb.148.5.925.

Muñiz, M., and Riezman, H. (2016). Trafficking of glycosylphosphatidylinositol anchored proteins from the endoplasmic reticulum to the cell surface. J. Lipid Res. *57*, 352–360. https://doi.org/10.1194/jlr.R062760.

Nakatsukasa, K. (2021). Potential physiological Relevance of ERAD to the biosynthesis of GPI-anchored proteins in yeast. Int. J. Mol. Sci. *22*, 1061. https://doi.org/10.3390/ijms22031061.

Phillips, B.P., Gomez-Navarro, N., and Miller, E.A. (2020). Protein quality control in the endoplasmic reticulum. Curr. Opin. Cell Biol. *65*, 96–102. https://doi.org/10.1016/j.ceb.2020.04.002.

Pinto, S.N., Silva, L.C., Futerman, A.H., and Prieto, M. (2011). Effect of ceramide structure on membrane biophysical properties: the role of acyl chain length and unsaturation. Biochim. Biophys. Acta *1808*, 2753–2760. https://doi.org/10.1016/j.bbamem.2011.07.023.

Ram, A.F., Wolters, A., Ten Hoopen, R., and Klis, F.M. (1994). A new approach for isolating cell wall mutants in Saccharomyces cerevisiae by screening for hypersensitivity to calcofluor white. Yeast *10*, 1019–1030. https://doi.org/10.1002/yea.320100804.

Reggiori, F., Canivenc-Gansel, E., and Conzelmann, A. (1997). Lipid remodeling leads to the introduction and exchange of defined ceramides on GPI proteins in the ER and Golgi of Saccharomyces cerevisiae. EMBO J. *16*, 3506–3518. https://doi.org/10.1093/emboj/16.12.3506.

Rodriguez-Gallardo, S., Kurokawa, K., Sabido-Bozo, S., Cortes-Gomez, A., Ikeda, A., Zoni, V., Aguilera-Romero, A., Perez-Linero, A.M., Lopez, S., Waga, M., et al. (2020). Ceramide chain length-dependent protein sorting into selective endoplasmic reticulum exit sites. Sci. Adv. *6*, eaba8237. https://doi.org/10.1126/sciadv.aba8237.

Satpute-Krishnan, P., Ajinkya, M., Bhat, S., Itakura, E., Hegde, R.S., and Lippincott-Schwartz, J. (2014). ER stress-induced clearance of misfolded GPI-anchored proteins via the secretory pathway. Cell *158*, 522–533. https://doi.org/10.1016/j.cell.2014.06.026.

Sikorska, N., Lemus, L., Aguilera-Romero, A., Manzano-Lopez, J., Riezman, H., Muñiz, M., and Goder, V. (2016). Limited ER quality control for GPI-anchored proteins. J. Cell Biol *213*, 693–704. https://doi.org/10.1083/jcb.201602010.

Sun, Z., and Brodsky, J.L. (2019). Protein quality control in the secretory pathway. J. Cell Biol. *218*, 3171–3187. https://doi.org/10.1083/jcb.201906047.

Takida, S., Maeda, Y., and Kinoshita, T. (2008). Mammalian GPI-anchored proteins require p24 proteins for their efficient transport from the ER to the plasma membrane. Biochem. J. *409*, 555–562. https://doi.org/10.1042/BJ20070234.

Tanaka, S., Maeda, Y., Tashima, Y., and Kinoshita, T. (2004). Inositol deacylation of glycosylphosphatidylinositol-anchored proteins is mediated by mammalian PGAP1 and yeast Bst1p. J. Biol. Chem. *279*, 14256–14263. https://doi.org/10.1074/jbc.M313755200.

Umemura, M., Fujita, M., Yoko-O, T., Fukamizu, A., and Jigami, Y. (2007). Saccharomyces cerevisiae CWH43 is involved in the remodeling of the lipid moiety of GPI anchors to ceramides. Mol. Biol. Cell *18*, 4304–4316. https://doi.org/10.1091/mbc.e07-05-0482.

Ventura, A.E., Varela, A.R.P., Dingjan, T., Santos, T.C.B., Fedorov, A., Futerman, A.H., Prieto, M., and Silva, L.C. (2020). Lipid domain formation and membrane shaping by C24-ceramide. Biochim. Biophys. Acta Biomembr *1862*, 183400. https://doi.org/10.1016/j.bbamem.2020.183400.

Yoko-O, T., Ichikawa, D., Miyagishi, Y., Kato, A., Umemura, M., Takase, K., Ra, M., Ikeda, K., Taguchi, R., and Jigami, Y. (2013). Determination and physiological roles of the glycosylphosphatidylinositol lipid remodelling pathway in yeast. Mol. Microbiol. *88*, 140–155. https://doi.org/10.1111/mmi.12175.

Yoko-O, T., Umemura, M., Komatsuzaki, A., Ikeda, K., Ichikawa, D., Takase, K., Kanzawa, N., Saito, K., Kinoshita, T., Taguchi, R., and Jigami, Y. (2018). Lipid moiety of glycosylphosphatidylinositol-anchored proteins contributes to the determination of their final destination in yeast. Genes Cells *23*, 880–892. https://doi.org/10.1111/gtc.12636.

Zanolari, B., Friant, S., Funato, K., Sütterlin, C., Stevenson, B.J., and Riezman, H. (2000). Sphingoid base synthesis requirement for endocytosis in Saccharomyces cerevisiae. EMBO J. *19*, 2824–2833. https://doi.org/10.1093/emboj/19.12.2824.

Zelnik, I.D., Ventura, A.E., Kim, J.L., Silva, L.C., and Futerman, A.H. (2020). The role of ceramide in regulating endoplasmic reticulum function. Biochim. Biophys. Acta Mol. Cell Biol Lipids *1865*, 158489. https://doi.org/10.1016/j.bbalip.2019.06.015.

STAR★METHODS

KEY RESOURCES TABLE

REAGENT or RESOURCE	SOURCE	IDENTIFIER
Antibodies		
rabbit anti-CPY	Custom generated antibody, a gift from H. Riezman	N/A
rabbit anti-Gas1	Custom generated antibody, a gift from H. Riezman	N/A
Chemicals, peptides, and recombinant proteins		
GFP-Trap Agarose Kit	Chromotek	gtak-20
Digitonin	Calbiochem	11024-24-1
Myriocin	Cayman Chemical	35891-70-4
Phosphatidylinositol-Specific Phospholipase C	Thermo Fisher Scientific	P6466
Trypsin Protease	Thermo Fisher Scientific	90057
Inositol, myo[2-3H(N)]	American Radiolabeled Chemicals	ART0116
TLC Silica gel 60, 25 Aluminium sheets	Merck	1.05553.0001
Deposited data		
MS data	This paper	ProteomeXchange Consortium (via jPOST partner repository): JPST001541/PXD032852
Experimental models: Organisms/strains		
For all strains of *S. cerevisiae*, see Table S1		
Recombinant DNA		
For all plasmids, see Table S2		

RESOURCE AVAILABILITY

Lead contact

Further information and requests for resources should be directed to and will be fulfilled by the Lead Contact, Kouichi Funato (kfunato@hiroshima-u.ac.jp).

Materials availability

Yeast strains and other unique/stable reagents generated in this study are available from the lead contact with a completed materials transfer agreement.

Data and code availability

Mass spectrometry data have been deposited to the ProteomeXchange Consortium via the jPOST partner repository. Data are publicly available as of the date of publication. The accession number is listed in the key resources table.

This paper does not report original code.

Any additional information required to reanalyze the data reported in this paper is available from the lead contact upon request.

EXPERIMENTAL MODELS AND SUBJECT DETAILS

Yeast strains

All strains of *S. cerevisiae* used for this work are listed in Table S1. Double mutants were constructed by crossing haploid yeast strains containing single-gene mutations in same backgrounds, sporulation and subsequent dissection of the spores. The genotypes of spores were verified by colony PCR.

METHOD DETAILS

Plasmids

All plasmids used for this work are listed in Table S2.

Culture conditions

Strains were grown either in rich YP medium (1% yeast extract, 2% peptone) supplemented with 0.2% adenine and containing either 2% glucose (YPD), 2% raffinose (YPR) or 2% galactose (YPG) as carbon source or in synthetic minimal medium (0.15% yeast nitrogen base, 0.5% ammonium sulfate) supplemented with the appropriate amino acids and bases as nutritional requirements, and containing either 2% glucose (SD) or 2% galactose (SG) as carbon source.

Immunoblotting

Cell lysates denatured with SDS sample buffer were separated by SDS-PAGE followed by immunoblotting (Manzano-Lopez et al., 2015; Ikeda et al., 2016). Blots were probed with rabbit polyclonal antibodies against Gas1, CPY, Emp24 and GFP, or rat monoclonal antibody against HA (3F10) and detected by chemiluminescence using peroxidase-conjugated affinity-purified goat anti-rabbit IgG or anti-rat IgG antibodies.

Fluorescence microscopy

Fluorescence observation by conventional fluorescence microscopy or super-resolution confocal live imaging microscopy (SCLIM) was performed as described (Manzano-Lopez et al., 2015; Rodriguez-Gallardo et al., 2020). For conventional fluorescence microscopy of Gas1-GFP, Mid2-Venus and Ted1-Venus, cells expressing Gas1-GFP, Mid2-Venus or Ted1-Venus were grown to log phase overnight in YPD, collected by centrifugation, and washed twice with phosphate-buffered saline. The cells were then incubated at least 15 min on ice before being examined by microscopy as described previously (Rodriguez-Gallardo et al., 2020). For visualization of Gas1-GFP clusters and into ERES, temperature-sensitive *sec31-1* mutant cells expressing galactose-inducible cargos (Gas1-GFP and/or Mid2-iRFP) and constitutive ERES marker Sec13-mCherry were grown to log phase overnight in YPR. After induction for 1 h at 24°C in YPG, cells were incubated for 30 min at 37°C in SG, shifted down to 24°C for releasing secretory block, imaged by conventional fluorescence microscopy or SCLIM, and analyzed with Volocity software as described (Rodriguez-Gallardo et al., 2020).

Native coimmunoprecipitation

Native coimmunoprecipitation experiment was performed as described (Rodriguez-Gallardo et al., 2020). The ER-enriched fraction was solubilized by treatment with 1% digitonin for 1h at 4°C and immunoprecipitated with GFP-Trap beads (Chromo Tek). The immunoprecipitated GFP protein complexes were separated by SDS-PAGE and analyzed by immunoblot.

MS analysis of GPI-glycan

MS analysis of GPI-glycan of Gas1-GFP was carried out exactly as described (Rodriguez-Gallardo et al., 2020). After treatment of Gas1-GFP with PI-PLC, immunoprecipitation with GFP-Trap, separation by SDS-PAGE, staining with Coomassie brilliant blue, and in-gel digestion with trypsin, the peptides carrying GPI-glycan were subjected to HPLC/mass spectrometry. MS and MS/MS data were obtained in positive ion mode over the mass range mass/charge ratio (m/z) 300 to m/z 3,000 by LTQ Orbitrap XL.

Lipid labelling with [^{3}H]*myo*-Inositol

In vivo labelling of lipids with [^{3}H]*myo*-inositol was carried out as described (Ikeda et al., 2021). Radiolabeled lipids were extracted with chloroform-methanol-water (10:10:3, vol/vol/vol), and analyzed by thin-layer chromatography using a solvent system (chloroform-methanol-0.25% KCl (55:45:10, vol/vol/vol)) for complex sphingolipids. Radiolabeled complex sphingolipids were visualized and quantified on an FLA-7000 system.

Pulse-chase analysis

Pulse-chase analysis of Gas1 with [^{35}S]methionine was performed as described previously (Kajiwara et al., 2008). After pulse-labeled and chased, the samples immunoprecipitated with anti-Gas1p rabbit antiserum and protein A-Sepharose were separated by SDS-PAGE and analyzed with a Phosphor Imager.

QUANTIFICATION AND STATISTICAL ANALYSIS

Statistical analysis

Statistical analysis was performed using Student's t-Test (n.s. not significant; *, $p < 0.05$; **, $p < 0.01$ and ***, $p < 0.001$). The mean ± s. d. for three independent experiments is shown.